Biosensors and Bioelectronics 141 (2019) 111416

Contents lists available at ScienceDirect

Biosensors and Bioelectronics

journal homepage: www.elsevier.com/locate/bios

Recent advances in biosensor for detection of lung cancer biomarkers

Gaojian Yang[a], Ziqi Xiao[a], Congli Tang[a], Yan Deng[a,b,*], Hao Huang[a], Ziyu He[a]

[a] Hunan Key Laboratory of Biomedical Nanomaterials and Devices, Hunan University of Technology, Zhuzhou, 412007, PR China
[b] State Key Laboratory of Bioelectronics, National Demonstration Center for Experimental Biomedical Engineering Education (Southeast University), School of Biological Science and Medical Engineering, Southeast University, Nanjing, 210096, PR China

ARTICLE INFO

Keywords:
Lung cancer
Tumor markers
Biosensors
Detection

ABSTRACT

Lung cancer is primary cancer threatening human life worldwide with the highest mortality rate. The early detection of lung cancer plays a critical role in the early diagnosis and subsequent treatment. However, the conventional methodologies limit the applications due to the low sensitivity, being expensive, and invasive procedure. Tumor markers as biochemical parameters can reflect cancer occurrence and progression, which show sensitivity, convenience, and low cost in developing biosensors, and act as good candidates for fabricating biosensors of detecting lung cancer. This review describes various biosensors (2013-2019) for detection of lung cancer biomarkers. Firstly, the various reported tumor markers of lung cancer are briefly described. Then, the advancements of designing biosensors for sensitive, stable, and selective identification of lung cancer biomarkers are systematically provided, with a specific focus on the main clinical biomarkers such as neuron-specific enolase (NSE), cytokeratin 19 fragment (CYFRA 21-1). Finally, the recent challenges and further opportunities for developing effective biosensors for early diagnosis of lung cancer are discussed.

1. Introduction

Nowadays, lung cancer is the most frequently life-threatening disease and still the prominent cause of cancer-related mortality among human beings worldwide (Torre et al., 2015). Conventionally, small cell lung cancer (SCLC) and non-small-cell lung cancer (NSCLC) are two major subtypes of lung cancer. The NSCLC has three histological types: large cell carcinoma, adenocarcinoma, and squamous cell carcinoma (Spira and Ettinger, 2004). SCLC accounts for about 20% of malignancy of lung cancer and has a poorer prognosis than NSCLC (Stupp et al., 2004). The genetic and epigenetic alterations make tumorigenic transformation and malignancy, which cause the complexity of lung cancer as a multistage disease (Bhatt et al., 2010). Due to the poor diagnosis and prognosis at the early stage, the mortality rate of lung cancer patients remains at a high level (Altintas et al., 2011).

The elevated levels of tumor markers can reflect cancer occurrence and progression, which are significantly associated with certain cancers in the diagnosis and clinical therapy (Arya and Shekhar, 2011; Liu et al., 2017; Yang et al., 2018). Thus, tumor markers as biochemical parameters provide a useful and dynamic approach to comprehend the spectrum of cancer with applications in screening, diagnosis, and prognosis (Kumar et al., 2008). Some tumor markers have become the vital monitoring targets for adjuvant therapy of lung cancer such as neuron-specific enolase (NSE) (Shibayama et al., 2001), cytokeratin 19 fragment (CYFRA 21-1) (Grenier et al., 1994), carcinoembryonic antigen (CEA) (Grunnet and Sorensen, 2012), squamous cell carcinoma antigen (SCCA) (Body et al., 1990), carcinoma antigen 125 (CA125) (Kimura et al., 1990), and tissue polypeptide antigen (TPA) (Buccheri and Ferrigno, 1988). However, the challenges of detecting elevated levels of tumor markers in plasma are significant due to the low level of tumor markers, high complexity of the biological system, and insufficient specificity which may cause false-positive results (Wu et al., 2007). Consequently, to find the novel lung cancer biomarkers (Altintas and Tothill, 2013; Miura et al., 2006) or to develop effective biosensors for biomarkers detection (Hyangah et al., 2009) can achieve early diagnosis and clinical therapy of lung cancer.

In the last decades, numerous methods for detecting lung cancer were developed, such as computed tomography (CT), chest radiograph (CRG), magnetic resonance imaging (MRI), positron emission tomography (PET), as well as a biopsy. However, these methods were extremely limited in screening lung cancer at early stages due to the low sensitivity, being expensive, and physical/chemical damage (Wang, 2017). Besides, though enzyme-linked immunosorbent assay (ELISA) and polymerase chain reaction (PCR) based methods have high sensitivity and less invasive procedures, there still exist the slow detection procedure and expensive consumption (Rusling et al., 2010). On this

* Corresponding author. Hunan Key Laboratory of Biomedical Nanomaterials and Devices, Hunan University of Technology, Zhuzhou, 412007, PR China.
E-mail address: hndengyan@126.com (Y. Deng).

https://doi.org/10.1016/j.bios.2019.111416
Received 2 April 2019; Received in revised form 28 May 2019; Accepted 4 June 2019
Available online 06 June 2019
0956-5663/

ground, various biosensors were designed for detecting lung cancer biomarkers, such as electrochemical biosensors (Chen et al., 2015; Liang and Liu, 2015; Liang et al., 2016), optical biosensors (Liu et al., 2016b), microfluidic biosensors (Gao et al., 2017a), microarrays biosensors (Gao et al., 2017b), and so on. Compared with the conventional methods, these novel biosensors exhibit better sensitivity, selectivity, stability, low cost, and easy operation in the complex samples (Ravalli et al., 2013). Moreover, with the rapid development of nanomaterials and biocompatible polymers, many ultrasensitive biosensors have been developed for the detection of lung cancer biomarkers (Arya and Shekhar, 2011). In this review, the reported lung cancer biomarkers are first summarized. Then, according to the main clinical lung cancer biomarkers, the advancements of designing biosensors for sensitive, stable, and selective identification of lung cancer biomarkers are systematically introduced. The fabricating strategies of biosensors are focused on electrochemical, optical, and point-of-care biosensors. Finally, the recent challenges and further opportunities for developing effective biosensors for early diagnosis of lung cancer are discussed.

2. Tumor markers of lung cancer

Tumor markers are biochemical parameters measured in the plasma or other body fluids from suspected patients of cancer, which have the nature of becoming a prerequisite for serologic tumor markers diagnosis (Henry and Hayes, 2012). The concentration of the tumor markers at any stage is determined by several parameters of the tumor, such as the size, mass, expression degree, synthesis ability, catabolic and excretion rates, as well as tumor blood supply (Akoun et al., 1985; Huang et al., 2010). Any variation of the factors will cause complexity and high sensitivity of the tumor markers detection. Tumor markers play an irreplaceable role for early detection and diagnosis of lung cancer in the current application. In the last decade, DNA methylation, a kind of highly sensitive and specific epigenetic biomarkers, is discovered and highlights pathological changes for lung cancer (Balgkouranidou et al., 2013). The following section concluded some significant tumor markers for lung cancer.

2.1. NSE

NSE is composed of two nearly identical polypeptide chains (α/γ or γ/γ), the molecular weight for both are 39 kDa. NSE is glycolytic enzyme enolase that is mainly found in the central and neuroendocrine tissues, peripheral neurons. In 1980, NSE has been reported to occur in SCLC, patients suffering from SCLC were observed to show a significantly high level of NSE (Qi et al., 2014). The release of the NSE may occur in erythrocyte and blood platelet, and change of its concentration is independent of age, sex, and smoking status (Schneider, 2006). The study by Ferrigno et al., (2003) indicated NSE was also a useful marker in NSCLC, as a predictor of survival independently of other prognostic factors. NSE has an obvious sensitivity and specificity for diagnosis and treatment of SCLC and also of clinical value in NSCLC.

2.2. CYFRA 21-1

CYFRA 21-1, a 36 kDa fragment of cytokeratin 19, locates in the cytoskeleton of epithelial cells (including bronchus epithelium) and is the only origin of CYFRA 21-1 providing high specificity. CYFRA 21-1 is proved to be exclusively expressed in lung tissues and the most sensitive tumor marker for NSCLC (particularly to squamous carcinoma) at present. Numerous multivariate analyses showed CYFRA 21-1 is an important marker in evaluating prognosis, treatment effect and recurrence of NSCLC (extremely in squamous carcinoma) (Ferrigno et al., 2003).

2.3. CEA

CEA, a molecular weight of about 180 kDa, is a cell membrane-associated glycoprotein group (Hammarström, 1999). The level of CEA is the highest in fetus serum of the 22 nd week of pregnancy (not in a healthy adult) (Ferrigno et al., 2003). In clinical diagnosis, CEA was regarded as a broad spectrum multi-tumor marker for detecting colon tumors, gastric, pancreatic, breast tumors, ovarian carcinoma, as well as lung carcinomas (Jiang et al., 2011). The normal range of CEA for a non-smoker and a smoker adult is less than 2.5 ng mL^{-1} and 5.0 ng mL^{-1}, respectively. The rise in CEA concentration shows the recurrence or the progression of lung cancer (Yuan et al., 2009). In exhaled breath condensate, a significantly higher concentration level of CEA indicates the best predictive characteristic of early-NSCLC (Zou et al., 2013). The diagnosis of lung malignancies is often combined CEA with CYFRA 21-1 (Okamura et al., 2013).

2.4. SCCA

SCCA is a 48-kDa protein belonging to the serine protease inhibitor family (Kato, 1992). The SCCA present in squamous cells and is regarded as a structural protein reflecting the differentiation stage of squamous cell cancers. Thus, changes in SCCA levels frequently show the extent of squamous carcinomas of the lung, cervix uteri, head and neck regions, and esophagus (Schneider, 2006). The changes in SCCA level were found closely relevant to the different stages of lung cancer. For monitoring NSCLC patients, SCCA determination was considered in combination with CYFRA21-1 (Kagohashi et al., 2008).

2.5. CA 125

CA 125, a 200-kDa membrane mucin-like glycoprotein, was recognized as a significant marker in monitoring the breast cancer, serous ovarian cancer, and lung cancer (Dai et al., 2014; Ferrigno et al., 2003). Significantly high serum level of CA 125 was mainly found in adenocarcinoma and large cell lung cancer and can be used as a predictive marker for evaluating the prognosis, the treatment effect, and the response of early treatment in NSCLC (Molina et al., 2003).

2.6. TPA

TPA, which belongs to the cytoskeleton protein with a molecular weight of 20 kDa (Buccheri and Ferrigno, 1988), was released by proliferating cells (originated from the cellular endoplasmic reticulum and cell membrane) (Nemoto et al., 1979). TPA is a sensitive, but low specific tumor marker for evaluation of lung cancer, as well as breast cancer (Buccheri et al., 1993). Moreover, TPA can show an independent and strong prognosis of lung cancer.

2.7. Others

In addition to the above commonly used markers for the detection of lung cancer, there are other biomarkers. These biomarkers, used to detect lung cancer, involve some of the interesting lung cancer biomarkers——Carbohydrate antigen 19-9 (Ghosh et al., 2012; Li et al., 2016a), tumor M2-pyruvate kinase (Tumor M2-PK), progastrin-releasing peptide (ProGRP), vascular endothelial growth factor (VEGF), serum human epididymis protein 4(HE4), cancer-testis antigen (NY-ESO-1); markers in a clinical application such as C-reactive protein (CRP), lactate dehydrogenase (LDH) (Ferrigno et al., 2003; Schneider, 2006); as well as newly discovered tumor markers of lung cancer——exosomal microRNA (Rabinowits et al., 2009), navitoclax (Gandhi et al., 2011), TFIIB-related factor 2 (Mehta et al., 2014), DR-70 (ArinÇ et al., 2016), glasgow prognostic score (Jiang et al., 2015), serum microRNA 21 (Sun et al., 2016), serum miR-204 (Guo et al., 2015), serum microRNA-100 (Jing et al., 2012), apurinic/apyrimidinic

endonuclease 1 (Jing et al., 2012), urokinase plasminogen activator (Almasi et al., 2013), etc. However, apart from the above serum markers, there are also markers of bronchoalveolar lavage fluid (such as ubiquitin specific peptidase 8, chitinase 3-like 1, and glutathione s-transferase P1) (Zhang et al., 2017), as well as breath markers (such as 2,4-dimethylheptane, 2-methyl-1-pentene, and 4-methyloctane) (Filipiak et al., 2014), which were also considered as potential marker of detecting lung cancer. Moreover, genomic and proteomic techniques have been used for molecular profiles of patients, and numerous protein biomarkers of lung cancer have been got (Zamay et al., 2017).

3. Biosensors of lung cancer markers detection

In the past years, a lot of rapid analysis strategies for lung cancer detection have been developed, such as electrochemical biosensors, optical biosensors, and so on. In the following, these biosensors will be systematically discussed, with a specific focus on the recent progress in NSE, CYFRA 21-1, CEA, SCCA, CA125, and TPA.

3.1. Biosensors of NSE detection

NSE shows strong specificity for SCLC (Tolan et al., 2013) and has been analyzed by electrochemical biosensors, optical biosensors, and surface-enhanced Raman scattering (SERS) biosensors. To detecting NSE, the electrochemical and optical analytical methods were most commonly used due to the high-sensitivity, rapidity, and simplicity. For achieving the higher and more stable signal amplification, lots of nanomaterials and polymers are applied to designing biosensors. In this part, strategies for developing biosensors for NSE detection were detailedly discussed.

3.1.1. Electrochemical biosensors

The electrochemical biosensors for NSE detection normally can be classified into labeled and label-free biosensors and can apply the nanomaterials and polymers for developing a sensitive platform. The labeled electrochemical biosensors commonly amplify detection signal based on the modified platform and labeled tag. Whereas label-free electrochemical biosensors only require a modified platform for signal amplification. For example, Wei et al., (2017) fabricated the electrochemical biosensors based on Au nanoparticles and reduced graphene oxide composites (Au NPs-rGO) signal amplification for NSE detection. In that work, the Au NPs-rGO provides numerous binding sites for modified antibody (Ab), and can remarkably enhance the signal of NSE detection. The biosensor showed a linear relationship from 0.1 to 2000 ng mL^{-1} and the limit of the detection (LOD) was 0.05 ng mL^{-1}. In order to achieve higher sensitivity, the 3D graphene (3D-GO) was used to design platform. As a paradigm, Fang et al., (2019) developed a novel electrochemical immunosensor using porous 3D graphene-starch architecture (3D-GNS) as a sensing platform and Au NPs coated ordered mesoporous carbon-silica (OMCSi-Au) as a target for NSE detection. The 3D-GNS and OMCSi-Au provided a higher surface area for the capture of target proteins and effective acceleration of electron transfer, and then the sensor displayed a lower LOD of 0.008 pg mL^{-1}.

Due to the more simplified sensing platform, the label-free electrochemical biosensors are commonly used to detect NSE and exhibit better stability. For example, Zhang and co-workers (Zhang et al., 2018) adopted 3D macroporous rGO/polyaniline film modified Au electrode for NSE detection. The 3DM rGO/PANI composite provided larger specific surface, high electron conductivity and electro-active sites for the NSE concentration detection. To further overcome the challenge of stability of the electrochemical biosensors, the molecular imprint (MIP) was served as artificial receptors for specifically recognizing target molecules. Wang et al., (2018b) reported a MIP-based electrochemical sensor with a 3D structured gold nanoarray as the amplification element and 1-(3-mercaptopropyl)-3-vinyl-imidazolium tetrafluoroborate as the molecularly imprinted film for NSE detection, when the NSE templates were removed. In the case of NSE detection, the linear response ranges from 0.01 to 1.0 ng mL^{-1} and a LOD of 2.6 pg mL^{-1}, with the relative standard deviations (RSD) less than 5.0%. For detecting the NSE in serum samples, Fan et al., (2017) developed a wireless point-of-care testing system using nanocomposites synthesized by Au NPs, thionine (Thi), and amino functional graphene as microfluidic paper-based analytical devices and smartphone as a signal receiver for NSE detection. The sensor showed a low LOD and wide detection range in serum samples, which has the promising potential of the clinical application.

3.1.2. Optical biosensors

Compared with electrochemical biosensors, the optical biosensors have less interference with the detection system, which is commonly used to detect biological target substances. Coupling with the development of optical and electrochemical methods, the photoelectrochemical (PEC) analyst methods are adapted to detect NSE more sensitively. For example, Li et al., (2017) described a PEC biosensor using 3D hyperbranched TiO_2 nanorod arrays as signal enhancers and dopamine (DA) as a sensitizer for NSE detection, with low LOD of 50 pg mL^{-1} in clinical serum samples. To effectively achieve point-of-care detection of NSE, Lin et al., (2019) developed an enzyme-free multicolor immunosensor for sensitive detection of NSE. The sensor adopted Cu^{2+}-modified carbon nitride nanosheets (Cu^{2+}-C_3N_4) as a catalytic substance and gold nanobipyramid (Au NBP) as the chromogenic substrate for multicolor display when the TMB^{2+} etches Au NPB to cause multicolor variations.

3.1.3. Other biosensors

The surface-enhanced Raman scattering (SERS) has been reported for immunosensing applications, with the modifiable surface for passivation or the conjugation of biomolecules. For example, Gao et al., (2017c) synthesized Au nanostar@malachite green isothiocyanate@silica nanoparticles (Au@MGITC@Si) as SERS probes. A novel SERS-based biosensor was fabricated by applying disposable paper-based lateral flow strip (PLFS) as a platform and Au@MGITC@Si as probes for the detection of NSE. The biosensor showed a wide detection range of 1–50000 ng mL^{-1} and LOD of 0.86 ng mL^{-1} in diluted blood plasma samples.

3.2. Biosensors of CYFRA 21-1 detection

CYFRA21-1, as the most effective biomarker of NSCLC, exhibits the high sensitivity and specificity. However, there are only a few relevant reports to apply CYFRA21-1 detection, including electrochemical and optical biosensors. In this section, the development of biosensors for CYFRA21-1 detection is discussed in detail.

3.2.1. Electrochemical biosensors

Based on assay approaches, the labeled electrochemical biosensors for CYFRA21-1 detection are firstly discussed. Zeng et al., (2018a) developed a novel labeled biosensor based on 3D-GO, chitosan (CS), and glutaraldehyde (GA) as a platform and Ab modified nanocomposites (synthesized by amino-functionalized carbon nanotube (MWCNT-NH_2), Thi, Au NPs, and horseradish peroxidase-labeled antibodies (HPR-Ab)) as a label for CYFRA21-1 detection. Due to the excellent conductivity and good biocompatibility of the nanomaterials, the biosensor exhibits fine linearity range of $0.1-150$ ng mL^{-1} and LOD of 43 pg mL^{-1} for detecting CYFRA21-1. As for label-free electrochemical biosensors for CYFRA21-1 detection, Gao et al., (2016) reported an immunosensor using silicon nanowire tunneling field-effect transistor (SiNW-TFET) where a “bottom-up” technique was adopted, that is, CMOS-compatibility and commercial production ability were incorporated into the biosensor for detecting CYFRA21-1 (Fig. 1). The “bottom-up” approach of tunneling-FET immunoassay can detect CYFRA21-1 concentrations as low as 0.65 fg mL^{-1}. Besides the conventional nanomaterials (Zeng

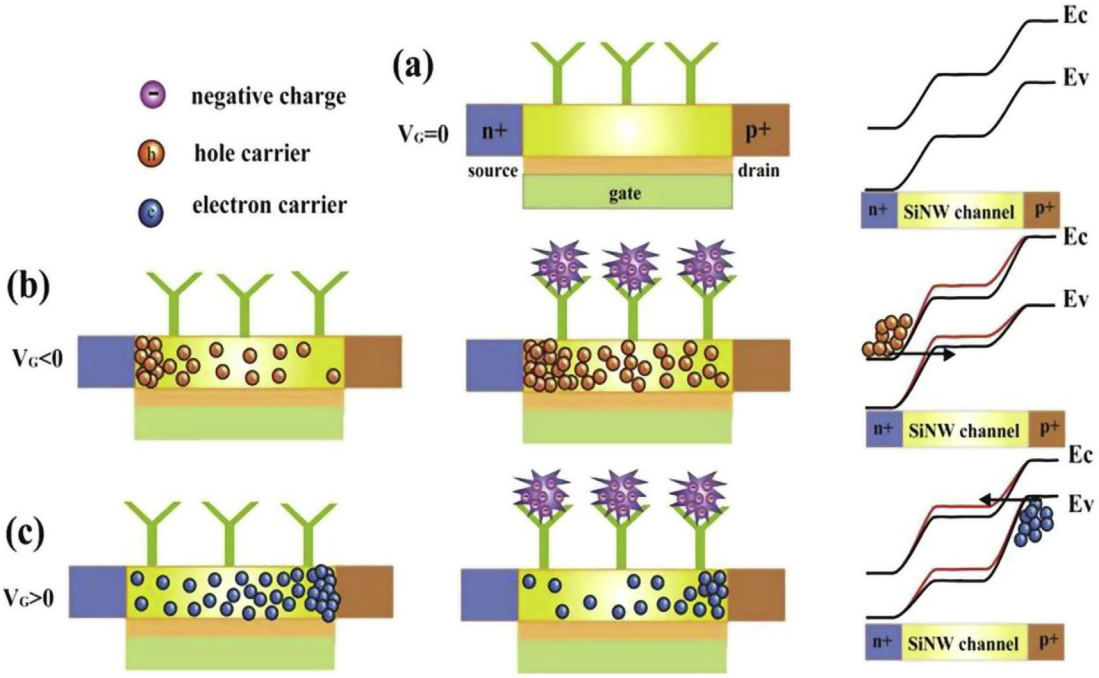

Fig. 1. Schematic illustration of the working principle of SiNW-TFET for detection of electrical charged biomolecules. The SiNW-TFET device was functioned with specific receptors and passivated with ethanolamine for biosensing. The details can be found in the Experimental Section. (a) In the off-state, the tunneling barrier between the channel and n+/p+ − doped source/drain regions is so large that tunneling is suppressed. (b) When V_G < 0 V, BTBT takes place at the channel/n + source tunneling junction. The bonding of negatively charged biomolecules further decreases the BTBT barrier (red line). This increases the tunneling current of SiNW-TFET. (c) When V_G > 0 V, the tunneling junction is between the channel and the p + drain region. This results in ambipolar conduction. The negatively charged biomolecule increases the BTBT barrier (red line) and reduces the tunneling current of the p-channel TFET. (Reproduced with permission from (Gao et al., 2016a) Copyright 2016, Macmillan Publishers Limited). (For interpretation of the references to color in this figure legend, the reader is referred to the Web version of this article.)

et al., 2018b), some novel materials (such as rare earth metal hydroxides and hydrogel) have been introduced for developing biosensors for CYFRA21-1 detection. According to the report by Tiwari et al., (2017), lanthanum hydroxide nanoparticles ($La(OH)_3$ NPs) were immobilized on an indium-tin-oxide glass substrate as a signal amplification platform, due to the better bioactive sites, high electron transfer mobility, and electrocatalytic behavior. The immunosensor exhibits high sensitivity for CYFRA21-1 detection, with a response time of 5 min. In another experiment, the conductive hydrogel can dramatically improve the detection sensitivity of amperometric biosensors, as reported in the work of Wang et al. (Wang and Ma, 2017), where an amperometric biosensor utilizing functionalized crosslinking phytic acid (containing Au NPs) was fabricated for detecting CYFRA21-1. The biosensor shows outstanding redox activity and electrons transfer capacity, which responses wide linear range of 50 fg mL^{-1}–100 ng mL^{-1} and LOD of 38 fg mL^{-1} for the CYFRA21-1 detection.

3.2.2. Optical biosensors

The utilization of optical immunoassay dramatically improved the sensitivity of CYFRA21-1 detection due to the low interference, low background nature, and high sensitivity. For example, Yu et al., (2019) described a novel PEC biosensor relying on biofunctional polydopamine/tungsten oxide nanocomposites (pDA/WO_3 NCs) as a sensing platform for CYFRA21-1 detection. The surface plasmon resonance (SPR) biosensors relied on the light-stimulated oscillation of electrons at the modifiable metal films, which can be directly used to detect the CYFRA21-1 (Chiu et al., 2018). In addition, the SPR-based biosensors exhibit excellent stability and high sensitivity for CYFRA21-1 detection in plasma samples. As a paradigm, Chiu et al., (2018) designed an ultrasensitive SPR immunosensor for detecting CYFRA21-1 based on cystamine (Cys) as a linker on the GO sheet immobilizing on the surface of the chip. The biosensor showed good properties of stability, sensitivity and the revealed kinetic fitted values in human plasma.

3.3. Biosensors of CEA detection

As a broad-spectrum tumor marker, the evaluation of CEA levels exhibits vital signs during the diagnosis, prognosis, and monitoring various cancer. Moreover, compared with other biomarkers, the larger molecular weight of CEA provides more functional groups for immobilization and modification. Thus, almost all the analytical methods have been developed for the detection of CEA, including electrochemical biosensors, optical biosensors, SPR-based biosensors, SERS-based biosensors, aptasensors, and so on. Here in the following part, the current progress of designing biosensors for CEA detection are briefly discussed.

3.3.1. Electrochemical biosensors

Recently, electrochemical biosensors have shown great application for CEA detection because of their fast response, stability, high sensitivity, and specificity. Besides, for achieving the signal amplification, various nanomaterials, such as noble metal nanomaterials, carbon nanomaterials, polymer nanomaterials, and so on, have been applied to design biosensors. In terms of labeled electrochemical biosensors, for example, Lee et al., (2017) fabricated a sandwich biosensor employing silver nanoparticles mixed with rGO (AgNPs-rGO) to modify screen-printed carbon electrode (SPCE) as sensing matrix and horseradish peroxidase-labeled Ab (HRP-Ab) as a tag for CEA detection. The sensor showed a calibration range of 0.05–0.50 μg mL^{-1} with a LOD of 35 ng mL^{-1}. Compared with enzymes, the nanomaterials commonly exhibit excellent stability, better sensitivity, and good modification. According to Feng et al., (2014), the Au NPs dotted thionine-functionalized carbon nanotubes (Thi-CNTs) and Au NPs doped polyaniline (PAN)-coated CNTs (Au NPs-PAN@CNTs) were applied for the

biosensor platform and signal label, respectively. That biosensor displayed high sensitivity towards CEA owing to the dual signal amplification of CNTs and AuNPs. In another work, Wang et al., (2018c) described a sensitive electrochemical immunoassay method for CEA detection relying on silver nanoparticles modified with molybdenum disulfide-coated Fe_3O_4 nanoparticles ($Ag/MoS_2@Fe_3O_4$) as a label and an analogous ELISA method. In this work, the Ab-conjugated $Ag/MoS_2@Fe_3O_4$ was selected through the ELISA and the detection was executed on magnetic glassy carbon electrode (MGCE) by using the selected label. The enzymes-like labeled electrochemical sensor possessed a low LOD of 0.03 pg mL^{-1}, which was lower than that of the work reported by Lee et al., (2017). Because of the development of systematic evolution of ligands by exponential enrichment (SELEX) method, aptamers as short single-stranded oligonucleotides (DNA or RNA) are widely applied to specifically recognize targets with high affinity, which display high specificity, higher stability, easy synthesis, and modification. As a paradigm, Xue et al., (2015) proposed an aptasensor based on "sandwich" tactics for sensitive detection of CEA. In that work, CEA aptamer 2 (CEAapt2), dendritic Pt@Au nanowires (Pt@AuNWs) and toluidine blue (Tb) formed Pt@AuNWs-CEAapt2-Tb bioconjugate (as a signal tag) and Au-decorated GCE immobilized with CEAapt1 (as sensing surface) was applied to capture the CEA to form sandwich-type construction. The novel sensor displayed good linear response to CEA in the range of 0.001–80 ng mL^{-1} with the LOD of 0.31 pg mL^{-1}.

For the label-free electrochemical biosensors of CEA detection, there have been various biosensors developed for CEA detection. For example, Shao et al., (2017) introduced a label-free immunoassay based on Prussian blue nanocubes loaded molybdenum disulfide nanocomposites (MoS_2-PBNCs) as a sensing platform for CEA detection (Fig. 2). The MoS_2-PBNCs possessed the excellent electrocatalytic ability, which could be applied to design a label-free biosensor for CEA detection in human serum with good expectation. Polymer nanomaterials display excellent redox-activity, easy modification, good biocompatibility, and stability, and have found applications in developed sensors for detecting CEA. According to the work of Ji et al. (Li et al., 2015), Au NPs-doped polydopamine (pDA) was utilized to modify carbon encapsulated Fe_3O_4 nanoparticles embedded in porous graphitic carbon nanocomposites (Fe_3O_4@C@PGC) as a platform for detection of CEA, which displayed low LOD of 0.33 pg mL^{-1} with the RSD of less than 3% (Fig. 3; Fig. 4). Based on polymers doping, Li et al., (2015) composited Au-F127 nanospheres as an electrochemical interface for the detection of CEA. To amplify the detection signal, the obtained Au-F127 nanospheres were applied for fabricating the label-free biosensor with the large surface, lots of active sites and high electron transfer. The biosensor had a wide calibration range of 0.001 − 10 ng mL^{-1} and LOD of 0.5 pg mL^{-1}.

3.3.2. Optical biosensors

Optical immunoassay, a classical immunoassay of CEA detection, has been widely applied for designing biosensors to enhance their stability, sensitivity, and antifouling. Danesh et al., (2018) exploited a fluorescent aptasensor for CEA detection based on 5,6,7-trimethyl-1,8-naphthyridin-2-amine (ATMND) as a fluorescent dye and three-way junction pocket as fluorescence quenching probe. According to the report, the CEAapt of three-way junction pocket was stripped in the presence of CEA. The aptsensor could effective detect CEA concentration and showed good recovery in human serum. Due to advantages (such as high sensitivity and simple operation) of upconversion nanoparticles (UCNPs), Wang et al., (2018a) developed a fluorescence resonance energy transfer (FRET) based immunosensor using fluorescein isothiocyanate (FITC) labeled (primary antibody) Ab_1 and Au NPs labeled (secondary antibody) Ab_2 to form Au NPs-CEA-FITC-Ab complex in the presence of CEA. The sensor exhibited color and fluorescence dual-readout due to Au NPs and FITC, which makes the analysis more universal and easier to use. Recently, the black phosphorus (BP), as a new member of the 2D layered materials family, exhibits attractive advantages of thickness-dependent direct bandgap, high charge carrier mobility, unique current on/off ratios, and excellent angle-dependent transport anisotropy (Hanlon et al., 2015), which has been developed for CEA detection. Peng et al., (2017) synthesized Au NPs-doped few-layer black phosphorus (BP-Au) as a versatile platform for sensitive label-free colorimetric detection of CEA due to the excellent catalytic activity and low activation energy of BP-Au. Later, the SERS, as spectroscopic tools for detecting CEA, integrated some advantages of high sensitivity, unique spectroscopic fingerprint, and nondestructive data acquisition. For example, Lin et al., (2016) developed a simple method to detect CEA in human serum relying on antibody-adsorbed Au and γ-Fe_2O_3@Au NPs as a probe, which exhibited a wide linear range of 1–50 ng mL^{-1} with LOD of 0.1 ng mL^{-1}. In addition, coupling with the development of electrochemical and optical techniques, some novel methodologies have been developed for CEA detection. Photoelectrochemical (PEC) biosensors, which can convert photoirradiation to an electrical signal, have been deemed a more effective assay for CEA analysis because of high sensitivity, low cost, and simple device. For example, Wu and co-workers (Wu et al., 2018) adopted $Zn_{0.1}Cd_{0.9}S$-hybridized g-C_3N_4 decorated indium-tin-oxide (ITO) slices as a photoactive matrix for accurate detection of CEA. The sensors showed high-intensity response and similar ultralow LOD due to the synergistic effect of the g-C_3N_4 and nanocomposites. Besides, the

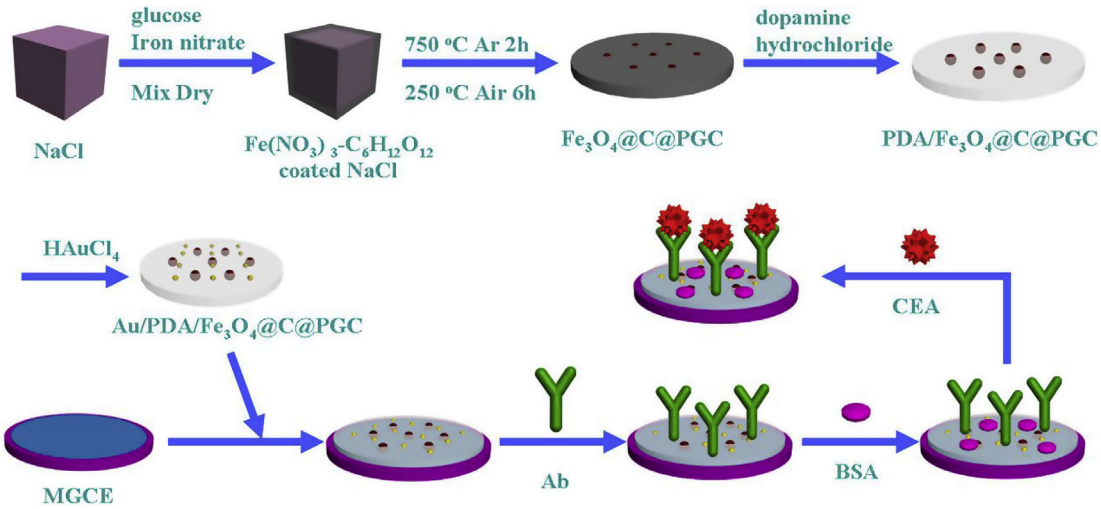

Fig. 2. The fabrication of the immunosensor. (Reproduced with permission from (Ji et al., 2016) Copyright 2016, Macmillan Publishers Limited).

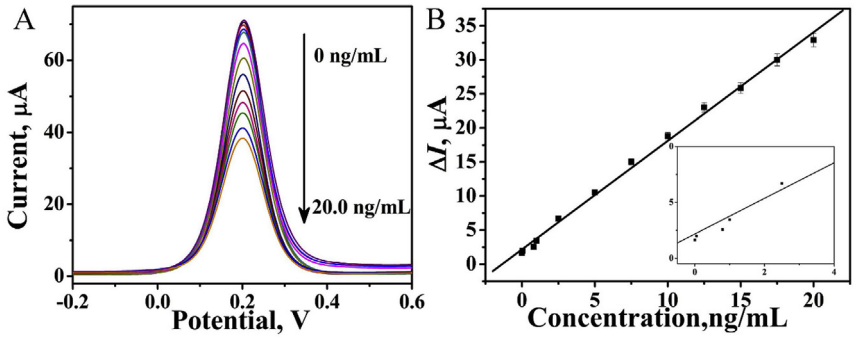

Fig. 3. The optimization of experimental conditions with Au/PDA/Fe_3O_4 @C@PGC concentration (A) and $K_4[Fe(CN)_6]$ concentration (B). (Reproduced with permission from (Ji et al., 2016) Copyright 2016, Macmillan Publishers Limited).

electrochemiluminescence (ECL) biosensors show high sensitivity and wide dynamic signal response range. As a paradigm, Pang et al., (2015) designed a label-free ECL sensor relying on graphene oxide/carboxylated multiwall carbon nanotubes/gold/cerium oxide nanoparticles (GO/MWCNTs-COOH/Au@CeO_2) as a sensing matrix for CEA detection due to the excellent electron transfer, good stability, and high specific surface area of the nanocomposites (Fig. 5).

3.3.3. Other biosensors

Besides, other immunoassays are also developed for CEA detection, and a few papers have been reported. For example, Chu et al., (2017) introduced a rapid and movable sensor based on FET for CEA detection. In that work, Ab-coated AlGaN/GaN high electron mobility transistors (HEMTs) acted as a detection matrix and showed good stability and excellent selectivity in human serum. In another work, Liu and co-workers (Liu et al., 2016a) reported an ultrasensitive lateral-flow immunoassay (LFIA) adopting magnetic nanoparticles (MNPs) as a probe for determination of CEA. For point-of-care CEA detection in human serum, Jiang et al., (2018) reported a novel rapid biosensor adopting glucose oxidase (GOx)-entrapped gold hollow microspheres (AuHMs) as a signal label for CEA detection, which used a portable pH meter to quantitatively determine the pH change effectively. With the GOx-AuHM labeling strategy, the biosensing device displayed an excellent analytical performance for CEA detection within good linear range and a low LOD of 0.062 ng mL^{-1}.

3.4. Biosensors of SCCA detection

The elevated level of SCCA was found in lung cancer, cervical squamous cell carcinoma, and hepatocellular carcinoma, which was used to monitor the progression of clinical therapy. Therefore, it is vital to develop available, sensitive, and rapid assays for the determination of SCCA. In the subsections below, the electrochemical and optical biosensors for SCCA detection were presented in detail, with a focus on the employed nanomaterials.

3.4.1. Electrochemical biosensors

The enzyme-mimetic nanomaterials were most commonly developed for designing electrochemical biosensors for SCCA detection, which were employed as labels of the antibody for achieving a reduction of hydrogen peroxide (H_2O_2) after the immuno-reaction. For example, Wang et al., (2014b) composited the Au@Ag@Au nanoparticles as enzyme-mimetic tags, with the nature of better stability and catalytic performance of H_2O_2. After the immune response, the biosensor showed a LOD of 0.18 pg mL^{-1} and a wide calibration curve from 0.5 pg mL^{-1} to 40 ng mL^{-1} for SCCA. To obtain better stability and sensitivity, Liu et al.,

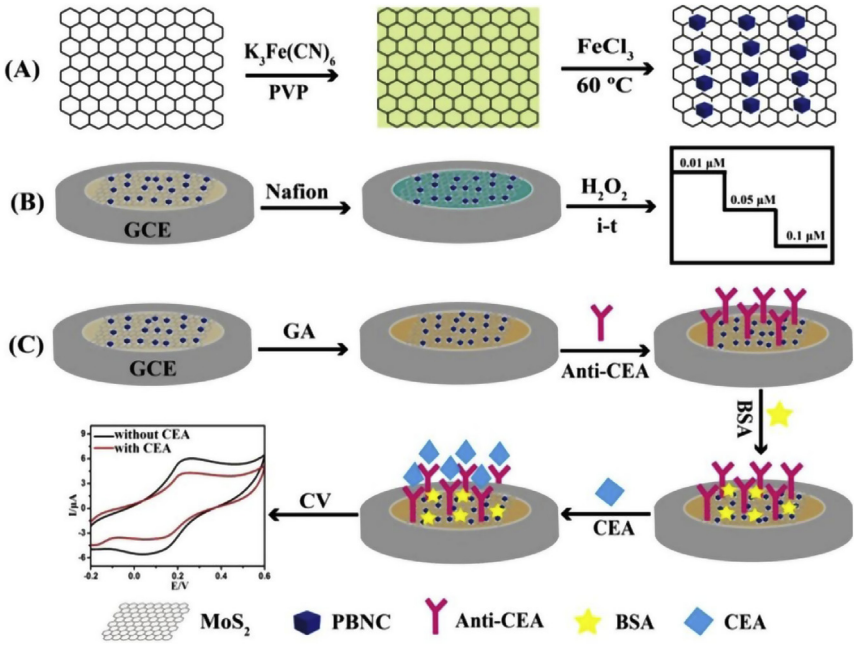

Fig. 4. (A) Schematic synthesis of MoS_2-PBNCs nanocomposite and illustration of MoS_2-based electrochemical sensors for (B) H_2O_2 and (C) CEA detection. (Reproduced with permission from (Shao et al., 2017) Copyright 2017, American Chemical Society.).

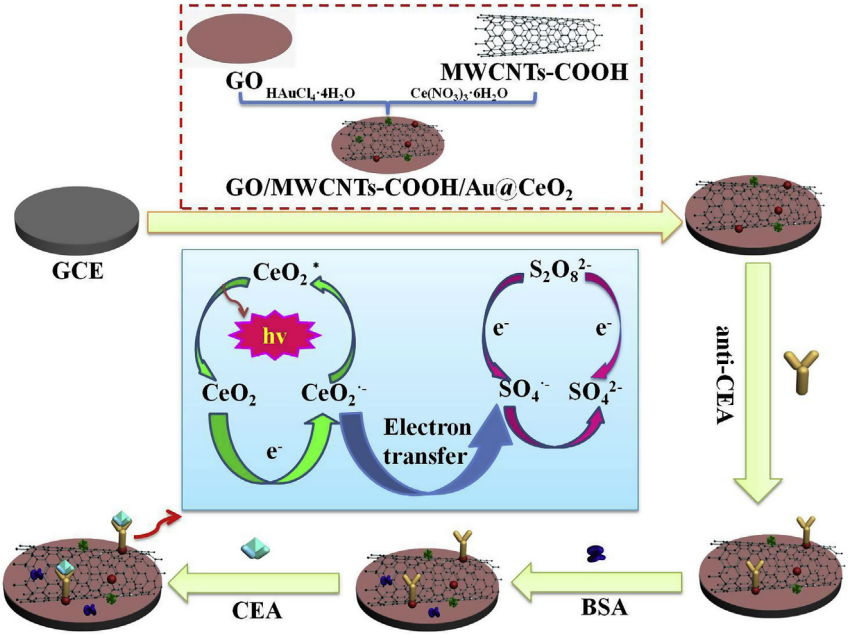

Fig. 5. Schematic diagram for fabrication of the label-free ECL immunosensor. (Reproduced with permission from (Pang et al., 2015) Copyright 2015, American Chemical Society).

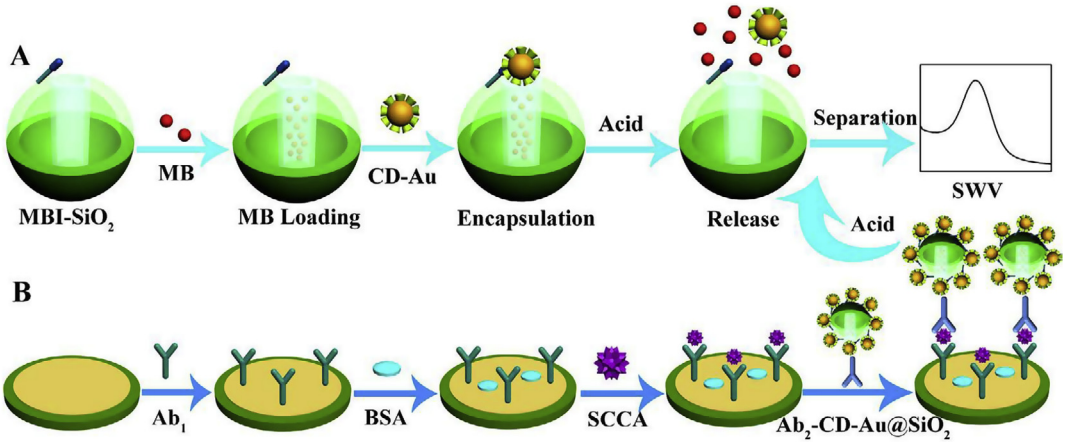

Fig. 6. Graphical representation of the pH responsive MS nanovalve (A) and the fabrication process of the immunosensor (B). (Reproduced with permission from (Ma et al., 2016) Copyright 2016, Macmillan Publishers Limited).

(2016c) synthesized different nanocomposites utilizing graphene to fabricate an ultrasensitive biosensor for detecting SCCA. According to the authors' results, β-cyclodextrin-loaded graphene sheet (CD-GS) as sensing platform due to the high supramolecular recognition of CD with GS (prevent stacking of GS and improve the biocompatibility of GS), and the ternary hollow Pt/PdCu nanocube (Pt/PdCu) anchored 3D graphene framework (Pt/PdCu-3DGF) as a sensitive label were applied. Besides, the controlled release system-based labeled biosensor was also fabricated to detect SCCA. For example, Ma et al. (Li et al., 2016b) designed a sample sandwich-type biosensor comprising of β-cyclodextrin functionalized gold decorated SiO_2 (CD-Au@SiO_2) as a tag and Ab_1 immobilized gold electrode (AuE) as a sensing platform for ultrasensitive detection of SCCA (Fig. 6). In that work, 1-methyl-1H-benzimidazole functionalized mesoporous SiO_2 (MBI-MS) was applied to encapsulate methylene blue (MB) with CD-Au@SiO_2 as a gatekeeper and entrapped the adamantly modified Ab_2 (ADA-Ab_2). The MB was released from MBI-MS in the acidic environment when the SCCA and functional Ab_2 achieve an immune reaction. The novel biosensor displayed good linear range from 0.001 to 20 ng·mL^{-1} with a low LOD of 0.25 pg·mL^{-1}.

For label-free electrochemical biosensors of SCCA detection, Li et al., (2016b) introduced a label-free biosensor for rapid detection of SCCA using icosahedral gold nanocrystals as carriers which were integrated to the Au NPs-decorated GCE by 1,3-di-(3-mercaptopropyl)-imidazolium bromide (DMIB). This novel biosensor using electrochemical analysis displayed a good response with the LOD of 12.6 pg mL^{-1} for SCCA. In another example, Gao et al., (2015) reported a label-free electrochemical sensor using Fe_3O_4 as a nanocontainer and aminated polystyrene microspheres (APSM) as a molecular gate to achieve encapsulation of toluidine blue (TB). The biosensor offered an amplified signal via square wave voltammetry (SWV) analysis for the released TB correlated with the amount of SCCA.

3.4.2. Optical biosensors

Recently, composite nanoparticles have become a hot topic for photoelectric immunosensors (such as ECL and PEC) due to their unique optical properties, electromagnetic feature, chemical stability, and mechanism of action. Wu et al., (2016a) fabricated magnetic graphene oxide (Fe_3O_4@GO) as a sensing matrix and Au NPs/g-C_3N_4 as a signal tag to form an "in-electrode"-type ECL biosensor for detecting SCCA.

Here, Fe_3O_4@GO can effectively capture Ab_1 to significantly amplify the detection signal, Au NPs/g-C_3N_4 not only enhance the loading capacity of Ab_2 but also provide a high conductivity to improve ECL intensity. Hence, the immunosensor displayed a wide range from 0.001 ng mL^{-1} to 10 ng mL^{-1} with a LOD of 0.4 pg mL^{-1}. Based on label-free PEC method, Ye et al., (2018) used $MoSe_2$ nanosheets with photocurrent intensity and hollow gold nanospheres (HGNs) as a sensing platform for detection of latent SCCA. This novel sensor exhibited a low LOD of 0.21 pg mL^{-1} for SCCA because the HGNs-$MoSe_2$ nanocomposite strengthened photocurrent intensity and improved binding site. For obtaining point-of-care detection of SCCA, Lin et al., (2018) designed a naked eyes-based colorimetric immunoassay for detection of SCCA using Au nanobipyramid@Ag nanorods (Au NBP@Ag) as carriers which were applied to modify Ab_2 and amplify detection signal. This fabricated sensor adopting colorimetric analysis showed a good linear response (2.5–105 ng mL^{-1}) with the low LOD (2.5 ng mL^{-1} for naked eyes and 0.85 ng mL^{-1} for spectrometer) for SCCA detection.

3.5. Biosensors of CA 125 detection

Change of concentration CA 125 provides an index for identifying the stage of lung cancer, which attracts the interest of researchers to detect the CA125 with limit level less than 35 U mL^{-1}. More details about the development of the biosensors for CA125 detection are provided in the following sections.

3.5.1. Electrochemical biosensors

In electrochemical immunoassays, numerous biosensors are fabricated for the detection of the CA125 due to the rapid, simple, easy-to-operate, and highly sensitive nature of the electrochemical methods. For example, Torati et al., (2016) introduced an innovative one-step electrochemical immunosensor for detection of CA125 using hierarchical gold nanostructures (GNs) as a platform which was applied to binding sites for CA125 and high electron transfer to amplify detection signal. This sensor adopting differential pulse voltammetry (DPV) analysis displayed an excellent linear response with the LOD of 5.5 U mL^{-1} for CA125. The incorporation of the polymer-metal complex such as PANI in conjugation with Au NPs and catalytic nanomaterials can enhance the sensitivity of amperometric biosensors, as introduced in the work by Zheng et al., (2017), where an amperometric immunosensor using AuNP-PB-PtNP-PANI nanocomposites were fabricated for the detection of CA125. The immunosensor showed its analytical response for CA125 in the dynamic detection range of 0.01–5000 U mL^{-1} and LOD of 4.4 mU mL^{-1}. In addition, the micro-flow assay was also applied to develop the biosensors for CA125 detection. Ravalli et al., (2016) reported a micro-flow biosensor for CA125 detection using thin-film modified gold array microelectrodes (IDAs). The authors electropolymerized anthranilic acid (AA) to IDAs as a simple sensing platform, which was applied to support and evaluate immunoreaction relying on electrochemical impedance spectroscopy (EIS). Although the EIS analysis simplified the complex transformation of detection, the method presented challenges of analysis of principle.

3.5.2. Optical biosensors

In another immunoassay of CA125 determination, the optical methods showed various advantages such as high sensitivity, wide detection range, low disturbance, and simple instrument. For example, Al-Ogaidi et al., (2014) fabricated a CL resonance energy transfer biosensor based on graphene quantum dots as a detecting platform and HRP-Ab_2 as a probe for detection of CA125. The immunosensor obtained an energy transfer between reactive oxygen species (the production of HRP-Ab_2 catalyzed H_2O_2) and luminol when the CA125 formed an immunocomplex with immobilized Ab_1 and HRP-Ab_2. Hence, the biosensor exhibited a wide detection range from 0.1 U mL^{-1} to 600 U mL^{-1} and a LOD of 0.05 U mL^{-1} for CA125. In fluorescence immunoassay, graphene quantum dots (GQDs) and carbon dots (CDs) are widely used in numerous immune tags for an increasing detection sensitivity of CA125 due to the excellent nature of the surface modification, biocompatibility, and stability against photobleaching. Tsai and researchers (Tsai et al., 2017) fabricated magnetic GQDs labeled with Ab_1 as a platform and fluorescent nanoparticles combined with Ab_2 as immumoprobe for CA125 detection. Moreover, according to Hosu and researchers (Hosu et al., 2017), a colorimetric smartphone-based immunoassay relying on detecting the grayscale value of sandwich-type immunocomplex (formed by Ab_1, CA125, and Ab_2-Au) stained by silver was designed for simplified detection of CA125.

3.5.3. Other biosensors

For lab-on-the-chip and point-of-care detection of CA125, Nunna et al., (2019) fabricated a novel biosensor for CA125 detection under microfluidic flow condition, conducting to understand the capacitive sensitivity of microfluidics-based biosensing mechanisms. Furthermore, other methods were also applied for the detection of CA125, such as FET and wavelength-dependent enhanced dark-field microscopy with dual-detection mode (EDFM-DM). Mansouri et al. (Mansouri and Salimi, 2018) introduced a flexible FET-type aptasensor adopting MWCNTs/rGO as a sensing platform for detecting CA125. Ju et al., (2017) reported an EDFM-DM sensor using silver nanoparticles (Ag NPs) as a fluorescence-free probe for CA125 detection. Both the biosensors showed a good linear range and low LOD for detecting CA125 in clinical samples and biological fluids.

3.6. Biosensors of TPA detection

As a single-chain polypeptide, TPA shows abnormal activity when a rapid increase presents in malignant tumors due to the production of TPA during the period of mitosis. Therefore, TPA as an auxiliary diagnosis is considered for lung cancer detection, which has been applied in developed sensors devoted to electrochemical assay for TPA detection. For example, Wang et al., (2014a) reported a sandwich-type biosensor relying on GS as a signal transfer platform, and Pd-Pt bimetallic nanocrystals labeled Ab_2 as a probe to catalyze H_2O_2 was applied, the sensitivity for the detection of TPA reached pg mL^{-1} level. According to the report, the Pd-Pt showed more excellent catalytic properties compared with any single nanocrystal and displayed higher stability than enzyme-tagged Ab_2. In another work, Wang and co-workers (Wang et al., 2016) synthesized multifunctional graphene nanocomposites (Au@MGN) based on Au NPs-absorbed nanoFe_3O_4@GO with the outstanding electrochemical property and biocompatibility. Then, a novel sensitive sandwich-type electrochemical immunosensor was designed by applying Au NPs modified GCE as a platform and Au@MGN as a probe for detecting TPA. The sensor showed a wide calibration range (10 fg mL^{-1}–100 ng mL^{-1}) and LOD (7.5 fg mL^{-1}) for TPA. Later, Wang et al., (2016) designed a general immunoassay adopting three-dimensional ordered macroporous gold films (3D-MGM) as a matrix and bifunctional, raspberry-like nano-raspberries (BiR-NRs) as labels for sensitive sensing of TPA. It was verified that BiR-NRs exhibited higher reduction peak current (compared with Au NPs and Pt NPs) due to properties of excellent electron transfer and strong catalytic activity for H_2O_2.

3.7. Biosensors of the others markers detections

Besides the conventional clinical detection of the biomarkers of lung cancer, the others for lung cancer detection have been discussed also. Base on this, the various biosensors for other biomarkers detection are integrated by different analysis strategies.

3.7.1. Electrochemical biosensors

According to the recent development of other biomarkers detection for lung cancer, the electrochemical assays were widely applied to

Table 1
A summary of developments of biosensors for lung cancer biomarkers.

Target	Method type	Linear range	Detection limit	RSD	Reference
NSE	electrochemical	20 fg mL^{-1}–35 ng mL^{-1}	8 fg mL^{-1}	2.3%	Fang et al. (2019)
NSE	electrochemical	0.5 pg mL^{-1}–10.0 ng mL^{-1}	0.1 pg mL^{-1}	3.7%	Zhang et al. (2018)
NSE	electrochemical	1 pg mL^{-1}–100 ng mL^{-1}	0.65 pg mL^{-1}	8.0%	Wang et al. (2018b)
NSE	optical	0.1–1000 ng mL^{-1}	50 pg mL^{-1}	≤9.5%	Li et al. (2017)
NSE	SERS	1–50000 ng mL^{-1}	0.86 ng mL^{-1}	≤7.0%	Gao et al. (2017c)
CYFRA21-1	electrochemical	0.1–150 ng mL^{-1}	43 pg mL^{-1}	6.4%	Zeng et al. (2018a)
CYFRA21-1	electrochemical	0.25–800 ng mL^{-1}	100 pg mL^{-1}	1.35%	Tiwari et al. (2017)
CYFRA21-1	optical	10 pg mL^{-1}–100 ng mL^{-1}	2.5 pg mL^{-1}	1.5%	Yu et al. (2019)
CEA	electrochemical	20 pg mL^{-1}–80 ng mL^{-1}	8 pg mL^{-1}	≤8.8%	Feng et al. (2014)
CEA	electrochemical	1 pg mL^{-1}–80 ng mL^{-1}	0.31 pg mL^{-1}	5.6%	Xue et al. (2015)
CEA	electrochemical	10 pg mL^{-1}–80 ng mL^{-1}	0.24 pg mL^{-1}	2.3%	Li et al. (2015)
CEA	optical	1–50 ng mL^{-1}	0.1 ng mL^{-1}	≤16.6%	Lin et al. (2016)
CEA	optical	5 pg mL^{-1}–20 ng mL^{-1}	1.4 pg mL^{-1}	≤3.2%	Wu et al. (2018)
CEA	optical	50 pg mL^{-1}–100 ng mL^{-1}	20 pg mL^{-1}	1.85%	Pang et al. (2015)
CEA	pH meter	0.1–100 ng mL^{-1}	62 pg mL^{-1}	≤11.6%	Liu et al. (2016a)
SCCA	electrochemical	0.5 pg mL^{-1} – 40 ng mL^{-1}	0.18 pg mL^{-1}	2.09%	Wang et al. (2014b)
SCCA	electrochemical	1 pg mL^{-1} – 4 ng mL^{-1}	0.33 pg mL^{-1}	≤5%	Gao et al., 2015a
SCCA	optical	1 pg mL^{-1} – 10 ng mL^{-1}	0.4 pg mL^{-1}	8.3%	Wu et al. (2016a)
SCCA	optical	1.0 pg mL^{-1} – 50 ng mL^{-1}	0.21 pg mL^{-1}	4.0%	Ye et al. (2018)
CA 125	electrochemical	10 mU mL^{-1}–5000 U mL^{-1}	4.4 mU mL^{-1}	≤3.5%	Zheng et al. (2017)
CA 125	electrochemical	0 U mL^{-1}–100 U mL^{-1}	7 U mL^{-1}	10%	Ravalli et al. (2016)
CA 125	optical	30 U mL^{-1}–1000 U mL^{-1}	30 U mL^{-1}	≤5%	Hosu et al. (2017)
CA 125	FET	1 nU mL^{-1}–1 U mL^{-1}	0.1 nU mL^{-1}	3.0%	Mansouri and Salimi (2018)
TPA	electrochemical	5 pg mL^{-1}–15 ng mL^{-1}	1.2 pg mL^{-1}	3.4%	Wang et al. (2014a)
TPA	electrochemical	10 fg mL^{-1}–100 ng mL^{-1}	7.5 fg mL^{-1}	1.68%	Wang et al. (2015)
TPA	electrochemical	1 pg mL^{-1}–15 ng mL^{-1}	0.7 pg mL^{-1}	4.8%	Wang et al. (2016)
VEGF	pH meter	0.8–480 pg mL^{-1}	0.5 pg mL^{-1}	–	Xu et al. (2017)
CEA; VEGF	electrochemical	CEA: 25–600 ng/mL; VEGF: 0.2–12.5 ng/mL	CEA: 4.31 ng/mL; VEGF: 14 pg/mL	3.33%	Kalyoncu et al. (2017)
NSE; CYFRA21-1; CEA; SCCA; CA 125	electrochemical	NSE: 1–150 ng·mL^{-1} CYFRA21-1: 1–150 ng·mL^{-1} CEA: 1–150 ng·mL^{-1} SCCA: 1–150 U·mL^{-1} CA 125: 0.1–100 ng·mL^{-1}	NSE: 0.9 ng·mL^{-1} CYFRA21-1: 0.4 ng·mL^{-1} CEA: 0.2 ng·mL^{-1} SCCA: 0.9 U·mL^{-1} CA 125: 30 pg·mL^{-1}	< 5%	Shan and Ma (2016)

design specific biosensors. For example, Yan et al., (2019b) developed a labeled electrochemical biosensor for HE4 detection in human serum samples. In that work, the graphene modified gold nanorods (Au NRs/NH_2-GS) as a platform and Au@Pd urchin-shaped nanostructures as a tag for realizing the quantitative detection of HE4. Due to the high specific surface area and good stability of the tag, the biosensor exhibits good linear range with low LOD. Later, Yan et al., (2019a) designed a label-free electrochemical biosensor based on Au@Pd holothurian-shaped nanoparticles (Au@Pd HSs) loaded on TiO_2 nanoclusters modified nitrogen-doped rGO (TiO_2-NGO) as a multi-amplification signal platform for HE4 detection, in which the lower LOD was obtained in real sample analysis.

3.7.2. Optical biosensors

Lots of optical biosensors have also been applied for other biomarkers detection of lung cancer. Qader et al., (2014) introduced a MIP based biosensor relying on peptide imprinted receptors for ProGRP detection. In that work, it has been verified that the peptide imprinted polymers were suitable for fabricating sensor platform for quantitative detection of ProGRP. Then, Piao and co-workers (Piao et al., 2019) developed an enzyme-free colorimetric biosensor based on complementary oligonucleotides of microRNA (miRNA) loaded SiO_2 microparticles (SiO_2 MPs) as the platform and a metal chelator decorated oligonucleotides as a probe for miRNA detection. The biosensor could quantitatively control the generation of Au NPs when the functionalized probe was immobilized on the platform. Besides, the ECL method, a phenomenon based on electroluminescent reactions, is another commonly applied method for the Apurinic/apyrimidinic endonuclease 1 (APE-1) detection. For instance, Zhao et al. (2014) reported a novel Ru $(bpy)_3^{2+}$/bi-arginine system to dramatically enhance the ECL efficiency of $Ru(bpy)_3^{2+}$, and then the ECL based biosensor was developed for APE-1 detection with an estimated LOD of 0.3 fg mL^{-1}.

3.7.3. Other biosensors

For achieving point-of-care detection, a large number of methods have been developed for other biomarkers of lung cancer. Xu et al., (2017) designed a biosensor based on pH meter/indicator for VEGF detection. In that work, the platform of immobilized Ab was applied to capture VEGF, and then the aptamer of VEGF was recognized. Next, the glucose oxidase (GOx)-functionalized ssDNAs hybridized with the aptamer to catalyze the oxidization of glucose for achieving VEGF detection.

3.8. Biosensors of the multiple detections

Commonly, the diagnosis of lung cancer should detect multiple tumor markers due to the complexity of pathogeny. Thus, it has been devoted to fabricating biosensors for effective, point-of-care, and rapid detection of lung cancer markers. For multilabel mode biosensors, the analytes should be effectively recognized by the specific activity of the labeled tags (such as nanomaterials or fluorescent dyes). For instance, Kalyoncu et al., (2017) synthesized γFe_2O_3 coated Au NPs-Pt NPs (AuPb@γFe_2O_3) and Au NPs-Cu NPs (AuCu@γFe_2O_3), and successfully employed the probes for simultaneous detection of CEA and VEGF. The proposed result revealed that good linearity from 0.2 ng mL^{-1} to 12.5 ng mL^{-1} and 25 ng mL^{-1} to 600 ng mL^{-1} for VEGF and CEA was obtained, respectively. To better achieve multiple detections, Shan et al. (Shan and Ma, 2016) designed an electrochemical biosensor based on nanomaterials and polymers for simultaneous detection of five markers of lung cancer. The biosensor adopting SWV analysis showed good detection range and low LOD for CEA, NSE, CA125, CYFRA21-1, and SCCA, respectively. Besides, Wu et al., (2016b) reported a fluorescence assay adopting multicolor QDs as signal tags and micro-magnetic beads as immune carriers for detection of three lung cancer markers because of differentiable emission maxima of three cross-talk-free QD

conjugated labels. The biosensor exhibited low LOD of 38 pg mL^{-1}, 364 pg mL^{-1}, 370 pg mL^{-1} for CEA, CYRFA 21-1, and NSE, respectively.

4. Conclusions and future perspectives

Various advanced techniques are integrated for fabricating biosensors for the early diagnosis of lung cancer, which is critical for clinical diagnosis and the early treatment of the patients. In recent years, great advancements have been seen in the field of the biosensor. In this brief review, the various reported tumor markers of lung cancer were first described briefly. Later, the development of designing biosensors for identification of the main clinical lung cancer biomarkers is systematically provided. The performance of these biosensors is shown in Table 1. Various sensitivity-enhancement techniques for these biosensors have been developed, and sensors showed a wide detection range and reduced the detection limit for biomarkers detection in lung cancer early diagnosis. In particular, the designing strategies of biosensors based on nanomaterials even provide signal amplified with several orders of magnitude for the determination of lung cancer biomarkers due to the accelerated signal transduction through a synergic effect among catalytic activity, conductivity, and biocompatibility. At the same time, the strategy for the simultaneous detection of multiple lung cancer markers (Gao et al., 2017b; Zhao et al., 2018) has been developed. However, for exact diagnosis of lung cancer, there are still many challenges needing to be overcome. Firstly, due to the high degree complexity of lung cancer cell, the reported biomarkers exhibit limitation for detecting early lung cancer. High sensitive and specific biomarkers are still pending discovery via genomic and proteomic profiling and further developing high sensitive detection methods such as biosensors for lung cancer detection. Secondly, due to the low concentration levels of lung cancer biomarkers, the sensitivity, specificity, and stability of biosensors are critical in the early diagnosis of lung cancer. The biosensors are fabricated using sensitivity-enhancement techniques by means of multifunctional nanomaterials. At the same time, the establishment of simultaneous detection of multiple biomarkers or dual-mode response detection method can greatly improve the diagnosis of lung cancer that needs multiplexed analysis. Finally, for clinical use, the biosensor development should devote to the capacity of resisting disturbance in whole blood. However, the bottlenecks for the detection of lung cancer biomarkers in whole blood are better stability, selectivity, portability, and low-power consumption. Therefore, for the biosensors, how to obtain better anti-disturbance property is very important, which can provide a novel chance for designing biosensors for accurate diagnosis of lung cancer in the clinic.

Declaration of interests

The authors declare that they have no known competing financial interests or personal relationships that could have appeared to influence the work reported in this paper.

CRediT authorship contribution statement

Gaojian Yang: Writing - original draft, Writing - review & editing, Conceptualization. **Ziqi Xiao:** Writing - review & editing. **Congli Tang:** Conceptualization. **Yan Deng:** Supervision, Writing - review & editing, Funding acquisition. **Hao Huang:** Conceptualization, Formal analysis. **Ziyu He:** Formal analysis.

Acknowledgments

This work was supported by the NSF of China (61871180), the National Key Research and Development Program of China (2018YFC1602905), China Postdoctoral Science Foundation (2016T90403), Postdoctoral Science Foundation of Jiangsu Province (1601021A), the Natural Science Foundation of Hunan Province (2017JJ2069), Hunan Provincial Innovation Foundation For Postgraduate (CX2018B745), and Hunan Key Research Project (2017SK2174) and Open Funding of State Key Laboratory of Oral Diseases (SKLOD2018OF02).

References

Akoun, G.M., Scarna, H.M., Milleron, B.J., Bénichou, M.R., Herman, D.R., 1985. Chest 87 (1), 39–43.
Al-Ogaidi, I., Gou, H., Aguilar, Z.P., Guo, S., Melconian, A.K., Al-Kazaz, A.K., Meng, F., Wu, N., 2014. Chem. Commun. 50 (11), 1344–1346.
Almasi, C.E., Drivsholm, L., Pappot, H., Hoyer-Hansen, G., Christensen, I.J., 2013. APMIS 121 (3), 189–196.
Altintas, Z., Tothill, I., 2013. Sens. Actuators B-Chem. 188, 988–998.
Altintas, Z., Uludag, Y., Gurbuz, Y., Tothill, I.E., 2011. Talanta 86, 377–383.
ArinÇ, S., KasapoĞLu, U.S., Akbay, Ö.M., OruÇ, Ö., Paker, N., 2016. Tuberk. ve Toraks 64 (1), 34–40.
Arya, S.K., Shekhar, B., 2011. Chem. Rev. 111 (11), 6783–6809.
Balgkouranidou, I., Liloglou, T., Lianidou, E.S., 2013. Biomark. Med. 7 (1), 49–58.
Bhatt, A.N., Mathur, R., Farooque, A., Verma, A., Dwarakanath, B.S., 2010. Indian J. Med. Res. 132 (8), 129–149.
Body, J.J., Sculier, J.P., Raymakers, N., Paesmans, M., Ravez, P., Libert, P., Richez, M., Dabouis, G., Lacroix, H., Bureau, G., 1990. Cancer 65 (7), 1552–1556.
Buccheri, G., Ferrigno, D., 1988. Chest 93 (3), 565–570.
Buccheri, G., Ferrigno, D., Vola, F., 1993. Lung Cancer 10 (1–2), 21–33.
Chen, M., Zhao, C., Xu, Q., Nie, B., Xu, L., Weng, S., Lin, X., 2015. Anal. Methods 7 (24), 10339–10344.
Chiu, N.F., Lin, T.L., Kuo, C.T., 2018. Sens. Actuators B-Chem. 265, 264–272.
Chu, C.H., Sarangadharan, I., Regmi, A., Chen, Y.W., Hsu, C.P., Chang, W.H., Lee, G.Y., Chyi, J.I., Chen, C.C., Shiesh, S.C., Lee, G.B., Wang, Y.L., 2017. Sci. Rep. 7 (1), 5256.
Dai, H., Liu, J., Liang, L., Ban, C., Jiang, J., Liu, Y., Ye, Q., Wang, C., 2014. Respirology 19 (5), 707–713.
Danesh, N.M., Yazdian-Robati, R., Ramezani, M., Alibolandi, M., Abnous, K., Taghdisi, S.M., 2018. Sen. Actuators, B. 256, 408–412.
Fan, Y., Liu, J., Wang, Y., Luo, J., Xu, H., Xu, S., Cai, X., 2017. Biosens. Bioelectron. 95, 60–66.
Fang, Y., Li, Y., Zhang, M., Cui, B., Hu, Q., Wang, L., 2019. Analyst 144, 2186–2194.
Feng, D., Li, L., Fang, X., Han, X., Zhang, Y., 2014. Electrochim. Acta 127, 334–341.
Ferrigno, D., Buccheri, G., Giordano, C., 2003. Lung Cancer 41 (3), 311–320.
Filipiak, W., Filipiak, A., Sponring, A., Schmid, T., Zelger, B., Ager, C., Klodzinska, E., Denz, H., Pizzini, A., Lucciarini, P., Jamnig, H., Troppmair, J., Amann, A., 2014. J. Breath Res. 8 (2), 027111.
Gandhi, L., Camidge, D.R., Ribeiro de Oliveira, M., Bonomi, P., Gandara, D., Khaira, D., Hann, C.L., McKeegan, E.M., Litvinovich, E., Hemken, P.M., Dive, C., Enschede, S.H., Nolan, C., Chiu, Y.L., Busman, T., Xiong, H., Krivoshik, A.P., Humerickhouse, R., Shapiro, G.I., Rudin, C.M., 2011. J. Clin. Oncol. 29 (7), 909–916.
Gao, A., Lu, N., Wang, Y., Li, T., 2016. Sci. Rep. 6, 22554.
Gao, A., Yang, X., Tong, J., Zhou, L., Wang, Y., Zhao, J., Mao, H., Li, T., 2017a. Biosens. Bioelectron. 91, 482–488.
Gao, J., Guo, Z., Yu, S., Su, F., Ma, H., Du, B., Wei, Q., Pang, X., 2015. Biosens. Bioelectron. 66, 141–145.
Gao, W., Wang, W., Yao, S., Wu, S., Zhang, H., Zhang, J., Jing, F., Mao, H., Jin, Q., Cong, H., Jia, C., Zhang, G., Zhao, J., 2017b. Anal. Chim. Acta 958, 77–84.
Gao, X., Zheng, P., Kasani, S., Wu, S., Yang, F., Lewis, S., Nayeem, S., Engler-Chiurazzi, E.B., Wigginton, J.G., Simpkins, J.W., Wu, N., 2017c. Anal. Chem. 89 (18), 10104–10110.
Ghosh, I., Bhattacharjee, D., Das, A.K., Chakrabarti, G., Dasgupta, A., Dey, S.K., 2012. Indian J. Clin. Biochem. 28 (1), 24–29.
Grenier, J., Pujol, J.L., Guilleux, F., Daures, J.P., Pujol, H., Michel, F.B., 1994. Nucl. Med. Biol. 21 (3), 471–476.
Grunnet, M., Sorensen, J.B., 2012. Lung Cancer 76 (2), 138–143.
Guo, W., Zhang, Y., Zhang, Y., Shi, Y., Xi, J., Fan, H., Xu, S., 2015. Int. J. Mol. Med. 36 (6), 1720–1726.
Hammarström, S., 1999. Semin. Canc. Biol. 9 (2), 67–81.
Hanlon, D., Backes, C., Doherty, E., Cucinotta, C.S., Berner, N.C., Boland, C., Lee, K., Harvey, A., Lynch, P., Gholamvand, Z., Zhang, S., Wang, K., Moynihan, G., Pokle, A., Ramasse, Q.M., McEvoy, N., Blau, W.J., Wang, J., Abellan, G., Hauke, F., Hirsch, A., Sanvito, S., O'Regan, D.D., Duesberg, G.S., Nicolosi, V., Coleman, J.N., 2015. Nat. Commun. 6 (1), 1–11.
Henry, N.L., Hayes, D.F., 2012. Mol. Oncol. 6 (2), 140–146.
Hosu, O., Ravalli, A., Lo Piccolo, G.M., Cristea, C., Sandulescu, R., Marrazza, G., 2017. Talanta 166, 234–240.
Huang, K.J., Niu, D.J., Xie, W.Z., Wang, W., 2010. Anal. Chim. Acta 659 (1–2), 102–108.
Hyangah, C., Sangyeop, L., Wook, S.S., Chil Hwan, O., Jaebum, C., 2009. Anal. Chem. 81 (8), 3029–3034.
Ji, L., Yan, T., Li, Y., Gao, J., Wang, Q., Hu, L., Wu, D., Wei, Q., Du, B., 2016. Sci. Rep. 6, 21017.
Jiang, A.G., Chen, H.L., Lu, H.Y., 2015. BMC Canc. 15, 1–6.
Jiang, W., Yuan, R., Chai, Y., Mao, L., Su, H., 2011. Biosens. Bioelectron. 26 (5), 2786–2790.
Jiang, Y., Su, Z., Zhang, J., Cai, M., Wu, L., 2018. Analyst 143 (21), 5271–5277.
Jing, L., Lu, K.H., Liu, Z.L., Ming, S., Wei, D., Wang, Z.X., 2012. BMC Canc. 12 (1), 519.
Ju, S., Chakkarapani, S.K., Lee, S., Kang, S.H., 2017. Sens. Actuators B-Chem. 245, 1015–1022.

Kagohashi, K., Satoh, H., Ishikawa, H., Ohtsuka, M., Sekizawa, K., 2008. Med. Oncol. 25 (2), 187–189.
Kalyoncu, D., Tepeli, Y., Kirgoz, U.C., Buyrac, A., Anik, U., 2017. Electroanalysis 29 (12), 2832–2838.
Kato, H., 1992. Humana Press.
Kimura, Y., Fujii, T., Hamamoto, K., Miyagawa, N., Kataoka, M., Iio, A., 1990. Br. J. Canc. 62 (4), 676–678.
Kumar, S., Mohan, A., Guleria, R., 2008. Biomarkers 11 (5), 385–405.
Lee, S.X., Lim, H.N., Ibrahim, I., Jamil, A., Pandikumar, A., Huang, N.M., 2017. Biosens. Bioelectron. 89 (Pt 1), 673–680.
Li, H., Xiao, Q., Lv, J., Lei, Q., Huang, Y., 2017. Anal. Biochem. 531, 48–55.
Li, J., Xie, H., Liu, Y., Ren, H., Zhao, W., Huang, X., 2015. Talanta 144, 404–410.
Li, Y., Li, X., Shi, G., Wang, P., Ma, H., 2016a. Acta Med. Mediterr. 32, 1671.
Li, Y., Zhang, Y., Jiang, L., Chu, P.K., Dong, Y., Wang, P., 2016b. RSC Adv. 6 (9), 6932–6938.
Liang, G., Liu, X., 2015. Microchim. Acta 182 (13–14), 2233–2240.
Liang, G., Man, Y., Jin, X., Pan, L., Liu, X., 2016. Anal. Chim. Acta 936, 222–228.
Lin, Y., Kannan, P., Zeng, Y., Qiu, B., Guo, L., Lin, Z., 2019. Sens. Actuators B-Chem. 283, 138–145.
Lin, Y., Xu, G., Wei, F., Zhang, A., Yang, J., Hu, Q., 2016. J. Pharm. Biomed. Anal. 121, 135–140.
Lin, Y., Xu, S., Yang, J., Huang, Y., Chen, Z., Qiu, B., Lin, Z., Chen, G., Guo, L., 2018. Sens. Actuators, B 267, 502–509.
Liu, F., Zhang, H., Wu, Z., Dong, H., Zhou, L., Yang, D., Ge, Y., Jia, C., Liu, H., Jin, Q., Zhao, J., Zhang, Q., Mao, H., 2016a. Talanta 161, 205–210.
Liu, L.J., Wang, W., Huang, S.Y., Hong, Y., Li, G., Sheng, L., Tian, J., Cai, Z., Wang, H.M.D., Ma, D.L., 2017. Chem. Sci. 8 (7), 4756–4763.
Liu, W., Zhang, A., Xu, G., Wei, F., Yang, J., Hu, Q., 2016b. J. Pharm. Biomed. Anal. 117, 18–25.
Liu, Y., Ma, H., Gao, J., Wu, D., Ren, X., Yan, T., Pang, X., Wei, Q., 2016c. Biosens. Bioelectron. 79, 71–78.
Ma, H., Wang, Y., Wu, D., Zhang, Y., Gao, J., Ren, X., Du, B., Wei, Q., 2016. Sci. Rep. 6, 19797.
Mansouri, S.M., Salimi, A., 2018. Anal. Chim. Acta 1000, 273–282.
Mehta, K., Lu, M., Tian, H., Yue, W., Li, L., Li, S., Qi, L., Hu, W., Gao, C., Si, L., 2014. PLoS One 9 (2), e88032.
Miura, N., Nakamura, H., Sato, R., Tsukamoto, T., Harada, T., Takahashi, S., Adachi, Y., Shomori, K., Sano, A., Kishimoto, Y., Ito, H., Hasegawa, J., Shiota, G., 2006. Cancer Sci. 97 (12), 1366–1373.
Molina, R., Filella, X., Auge, J.M., Fuentes, R., Bover, I., Rifa, J., Moreno, V., Canals, E., Vinolas, N., Marquez, A., Barreiro, E., Borras, J., Viladiu, P., 2003. Tumour Biol 24 (4), 209–218.
Nemoto, T., Constantine, R., Chu, T.M., 1979. J. Nat. Cancer I. 63 (6), 1347–1350.
Nunna, B.B., Mandal, D., Lee, J.U., Zhuang, S., Lee, E.S., 2019. BioNanoScience 9 (1), 203–214.
Okamura, K., Takayama, K., Izumi, M., Harada, T., Furuyama, K., Nakanishi, Y., 2013. Lung Cancer 80 (1), 45–49.
Pang, X., Li, J., Zhao, Y., Wu, D., Zhang, Y., Du, B., Ma, H., Wei, Q., 2015. ACS Appl. Mater. Inter. 7 (34), 19260–19267.
Peng, J., Lai, Y., Chen, Y., Xu, J., Sun, L., Weng, J., 2017. Small 13 (15), 1–11.
Piao, J., Zhao, Q., Zhou, D., Peng, W., Gao, W., Chen, M., Shu, G., Gong, X., Chang, J., 2019. Anal. Chim. Acta 1052, 145–152.
Qader, A.A., Urraca, J., Torsetnes, S.B., Tonnesen, F., Reubsaet, L., Sellergren, B., 2014. J. Chromatogr. A 1370, 56–62.
Qi, W., Li, X., Kang, J., 2014. J. Cancer Res. Ther. 10 (Suppl. l), C95–C101.
Rabinowits, G., Gercel-Taylor, C., Day, J.M., Taylor, D.D., Kloecker, G.H., 2009. Clin. Lung Cancer 10 (1), 42–46.
Ravalli, A., dos Santos, G.P., Ferroni, M., Faglia, G., Yamanaka, H., Marrazza, G., 2013. Sens. Actuators B-Chem. 179, 194–200.
Ravalli, A., Lozzi, L., Marrazza, G., 2016. Curr. Drug Deliv. 13 (3), 400–408.
Rusling, J.F., Kumar, C.V., Gutkind, J.S., Patel, V., 2010. Analyst 135 (10), 2496–2511.
Schneider, J., 2006. Adv. Clin. Chem. 42, 1–41.
Shan, J., Ma, Z., 2016. Microchim. Acta 183 (11), 1–9.
Shao, S., Han, X., Lu, Z., Wei, L., Dan, Z., Jie, C., Fan, C., Wang, L., Song, S., Weng, L., 2017. Acs Appl. Mater. Inter. 9 (14), 12773–12781.
Shibayama, T., Ueoka, H., Nishii, K., Kiura, K., Tabata, M., Miyatake, K., Kitajima, T., Harada, M., 2001. Lung Cancer 32 (1), 61–69.
Spira, A., Ettinger, D.S., 2004. N. Engl. J. Med. 350 (19), 379–392.
Stupp, R., Monnerat, C., Turrisi 3rd, A.T., Perry, M.C., Leyvraz, S., 2004. Lung Cancer 45 (1), 105–117.
Sun, M., Song, J., Zhou, Z., Zhu, R., Jin, H., Ji, Y., Lu, Q., Ju, H., 2016. Dis Markers 2016. pp. 3823121.
Tiwari, S., Gupta, P.K., Bagbi, Y., Sarkar, T., Solanki, P.R., 2017. Biosens. Bioelectron. 89 (Pt 2), 1042–1052.
Tolan, N.V., Vidal-Folch, N., Algeciras-Schimnich, A., Singh, R.J., Grebe, S.K., 2013. Clin. Chim. Acta 424, 216–221.
Torati, S.R., Kasturi, K.C.S.B., Lim, B., Kim, C.G., 2016. Sens. Actuators B-Chem. 243, 64–71.
Torre, L.A., Bray, F., Siegel, R.L., Ferlay, J., Lortet-Tieulent, J., Jemal, A., 2015. CA cancer. J. Clin. 65 (2), 87–108.
Tsai, H., Lin, W., Chuang, M., Lu, Y., Fuh, C.B., 2017. Biosens. Bioelectron. 90, 153–158.
Wang, H., Ma, Z., 2017. Microchim. Acta 184 (4), 1045–1050.
Wang, J., Cao, F., He, S., Xia, Y., Liu, X., Jiang, W., Yu, Y., Zhang, H., Chen, W., 2018a. Talanta 176, 444–449.
Wang, L., 2017. Sensors (Basel) 17 (10), 2420.
Wang, X., Wang, Y., Ye, X., Wu, T., Deng, H., Wu, P., Li, C., 2018b. Biosens. Bioelectron. 99, 34–39.
Wang, Y., Li, R., Zhang, X., Liu, Y., Wang, X., Zhang, S., Du, B., Wei, Q., 2016. J. Nanosci. Nanotechnol. 16 (12), 12275–12281.
Wang, Y., Wang, Y., Pang, X., Du, B., Li, H., Wu, D., Wei, Q., 2015. Sens. Actuators B-Chem. 214, 124–131.
Wang, Y., Wei, Q., Zhang, Y., Wu, D., Ma, H., Guo, A., Du, B., 2014a. Nanotechnology 25 (5), 055102.
Wang, Y., Zhang, Y., Su, Y., Li, F., Ma, H., Li, H., Du, B., Wei, Q., 2014b. Talanta 124, 60–66.
Wang, Y., Zhao, G., Zhang, Y., Pang, X., Cao, W., Du, B., Wei, Q., 2018c. Sens. Actuators B-Chem. 266, 561–569.
Wei, Z., Zhang, J., Zhang, A., Wang, Y., Cai, X., 2017. Molecules 22 (3), 392.
Wu, J., Fu, Z., Yan, F., Ju, H., 2007. TrAC Trends Anal. Chem. (Reference Ed.) 26 (7), 679–688.
Wu, L., Hu, Y., Sha, Y., Li, W., Yan, T., Wang, S., Li, X., Guo, Z., Zhou, J., Su, X., 2016a. Talanta 160, 247–255.
Wu, S., Liu, L., Li, G., Jing, F., Mao, H., Jin, Q., Zhai, W., Zhang, H., Zhao, J., Jia, C., 2016b. Talanta 156–157, 48–54.
Wu, T., Zhang, Y., Wei, D., Wang, X., Yan, T., Du, B., Wei, Q., 2018. Sens. Actuators B-Chem. 256, 812–819.
Xu, H., Kou, F., Ye, H., Wang, Z., Huang, S., Liu, X., Zhu, X., Lin, Z., Chen, G., 2017. Talanta 175, 177–182.
Xue, S., Yi, H., Jing, P., Xu, W., 2015. RSC Adv. 5 (94), 77454–77459.
Yan, Q., Cao, L., Dong, H., Tan, Z., Hu, Y., Liu, Q., Liu, H., Zhao, P., Chen, L., Liu, Y., Li, Y., Dong, Y., 2019a. Biosens. Bioelectron. 127, 174–180.
Yan, Q., Cao, L., Dong, H., Tan, Z., Liu, Q., Zhang, W., Zhao, P., Li, Y., Liu, Y., Dong, Y., 2019b. Anal. Chim. Acta 1069, 117–125.
Yang, G.J., Wang, W., Mok, S.W.F., Wu, C., Law, B.Y.K., Miao, X.M., Wu, K.J., Zhong, H.J., Wong, C.Y., Wong, V.K.W., 2018. Angew. Chem. Int. Edit. 57 (40), 13091–13095.
Ye, X., Li, M., Hu, Y., Wang, Z., Wang, Y., Deng, H., Xiong, X., Li, C., Sun, D., 2018. Sens. Actuators B-Chem. 275, 199–205.
Yu, Y., Huang, Z., Zhou, Y., Zhang, L., Liu, A., Chen, W., Lin, J., Peng, H., 2019. Biosens. Bioelectron. 126, 1–6.
Yuan, Y.R., Yuan, R., Chai, Y.Q., Zhuo, Y., Miao, X.M., 2009. J. Electroanal. Chem. 626 (1–2), 6–13.
Zamay, T.N., Zamay, G.S., Kolovskaya, O.S., Zukov, R.A., Petrova, M.M., Gargaun, A., Berezovski, M.V., Kichkailo, A.S., 2017. Cancers (Basel) 9 (11), 1–22.
Zeng, Y., Bao, J., Zhao, Y., Huo, D., Chen, M., Qi, Y., Yang, M., Fa, H., Hou, C., 2018a. Bioelectrochemistry 120, 183–189.
Zeng, Y., Bao, J., Zhao, Y., Huo, D., Chen, M., Yang, M., Fa, H., Hou, C., 2018b. Talanta 178, 122–128.
Zhang, Q., Li, X., Qian, C., Dou, L., Cui, F., Chen, X., 2018. Anal. Biochem. 540–541, 1–8.
Zhang, S., Zhao, Y.F., Zhang, M.Z., Wu, X.L., 2017. Clin. Respir. J. 11 (4), 481–488.
Zhao, L., Han, H., Ma, Z., 2018. Biosens. Bioelectron. 101, 304–310.
Zhao, M., Chai, X.D., Han, J., Gui, G.F., Yuan, R., Zhuo, Y., 2014. Anal. Chim. Acta 846, 36–43.
Zheng, Y., Wang, H., Ma, Z., 2017. Microchim. Acta 184 (11), 4269–4277.
Zou, Y., Wang, L., Zhao, C., Hu, Y., Xu, S., Ying, K., Wang, P., Chen, X., 2013. J. Breath Res. 7 (4), 047101.